Calculations of Vibrational Energy Levels by Using a Hybrid ab Initio and DFT Quartic Force Field: Application to Acetonitrile

D. Begue,† P. Carbonniere,‡ and C. Pouchan*

Laboratoire de Chimie Théorique et Physico-Chimie Moléculaire - UMR 5624, Fédération de Recherche IPREM 2606, Université de Pau et des Pays de l'Adour, IFR - Rue Jules Ferry, 64000 PAU, France

Received: September 15, 2004

A hybrid quartic force field with quadratic force constants calculated at the CCSD(T)/cc-pVTZ level and cubic and quartic terms determined by a B3LYP/cc-pVTZ treatment is proposed to compute the vibrational energy levels of acetonitrile from a variational method. Fundamentals and overtones calculated in the range of 300−3200 cm^{-1} are in fair agreement with the 31 observed data, with an absolute mean deviation of less than 0.8%. These results allow us to explain several Fermi resonances.

1. Introduction

During the past decade, several anharmonic force fields of molecular systems with 3−12 atoms[1−14] were calculated with methods well known to fit experimental data to within an average error of about 10 cm^{-1}. Among these methods, MRCI (multireference CI)[15,16] and CCSD(T) (coupled cluster singles and doubles including a perturbative estimation of connected triples)[17] were generally used for the investigation of tri- and tetra-atomic systems and were shown to further improve the accuracy mentioned above[18−20] when used with a triple-ζ or higher-quality basis set. For larger molecular systems, the anharmonic force field can be calculated by a Møller−Plesset perturbative method[21] or by the popular DFT (density functional theory) method.[22] These last two methods have shown their ability to account correctly, at lower cost, for the anharmonic constants[23−25] in the study of organic systems. These observations make it reasonable to expect that a combined way of determining the hybrid force fields,[7,13,26−27] where the structural parameters and the harmonic constants are calculated by using a CCSD(T) method, whereas the cubic and quartic force constants expressed in the basis of the normal CCSD(T) modes are determined by an MP2 or a DFT approach, could be suitable for the treatment of large-scale molecular systems.

This paper therefore presents the computed vibrational spectrum of acetonitrile because even though this molecule has been the subject of many experimental studies for the past 40 years no accurate quartic force field has yet been given theoretically. Earlier theoretical work addressed the optimization of the geometry and calculation of the quadratic force field as well as the Raman intensities.[28] The structure of CH_3CN was calculated by Margules et al.[29] by using MP2 and CCSD(T) methods with several Dunning basis sets.[30] The results obtained by these authors are in excellent agreement with the data deduced from experimental observations by Le Guennec et al.[31] The harmonic force field was calculated at both the HF/6-31+G-(d,p)[32] and MP2/cc-pVDZ[33] levels of theory and was given in a semiempirical approximation by Hedberg et al.,[34] as well as by fitting all of the force constants with the experimental data of Duncan et al.[35] Experimental data are, however, more numerous over the whole IR spectral range and concern the fundamental and overtone bands between 300 and 3100 cm^{-1},[1,35−37] the first overtone band of CH stretching modes,[38] and several Fermi interactions from high-resolution analysis.[39−55] These data constitute a significant source of information that will serve as a reference to evaluate the degree of accuracy of our quartic hybrid force field CCSD(T)//B3LYP, abbreviated below to (CC//B3). This approach should constitute a starting point for the future treatment of medium-size molecules for which it is, nowadays, difficult to use CCSD(T) or MRCI methods. In addition, the calculation of the CH_3CN vibrational spectrum in the mid-IR region would make it possible for the experimentalists to refine their vibrational assignment.

2. Method and Computational Details

All calculations were carried out using a Dunning correlation-consistent pVTZ Cartesian basis set[30] in our CCSD(T) and DFT approaches. The Becke[56] three-parameter exchange functional (B3) in combination with the Lee, Yang, and Parr[57] (LYP) correlation functional was used in our DFT calculations. Geometry optimization, energies, and analytical first derivatives were obtained by using the Gaussian 98 package.[58]

For each system of interest, the calculation of the molecular vibrations requires an analytical expression for the corresponding potential function. For systems in which symmetry is used and anharmonicity is small, one of the possible ways to describe modes or combinations of modes in the mid-IR region is to write this potential function as a Taylor expansion series in the space of the dimensionless normal coordinates q:

$$V_{\text{hybrid}} = \frac{1}{2!}\sum_i \varpi_{i_{\text{CCSD(T)}}} q_i^{\,2} + \frac{1}{3!}\sum_{i,j,k} \phi_{ijk_{\text{B3LYP}}} q_i q_j q_k + \frac{1}{4!}\sum_{i,j,k,l} \phi_{ijkl_{\text{B3LYP}}} q_i q_j q_k q_l \quad (1)$$

The dimensionless normal coordinate space is constructed from curvilinear coordinate space. Simons−Parr−Finlan coordinates[59] or Morse-like coordinates[60] can also be used for strongly anharmonic oscillators.

* Corresponding author. E-mail: claude.pouchan@univ-pau.fr.
† E-mail: didier.begue@univ-pau.fr.
‡ E-mail: philippe.carbonniere@univ-pau.fr.

10.1021/jp0406114 CCC: $30.25
Published on Web 04/30/2005

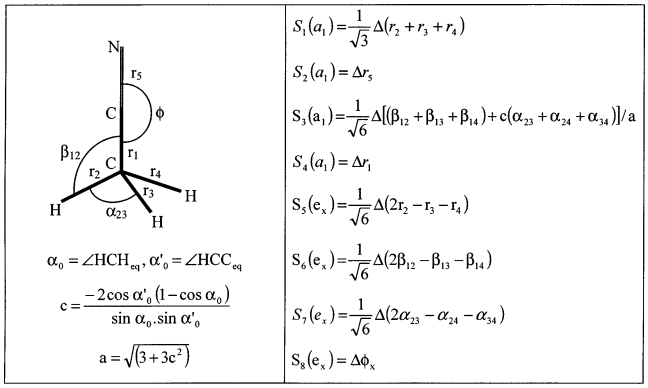

Figure 1. Internal and symmetry coordinates for CH_3CN.

In eq 1, $\varpi_{i\mathrm{CCSD(T)}}$ represents the harmonic wavenumbers expressed in cm^{-1}, calculated at the CCSD(T)/cc-pVTZ level. The quadratic force constants, which enable the calculation of the harmonic frequencies, are determined by linear regression on a twice-redundant grid of 49 points, which are calculated in the space of symmetry coordinates. The harmonic force field of CH_3CN can be completely described by just the four a_1 coordinates and the four e_x components of the doubly degenerate modes (Figure 1), taking into account the symmetry of the molecule and applying the Henri and Amat relations[61]

Let $\phi_{ijk_{\mathrm{B3LYP}}}$ and $\phi_{ijkl_{\mathrm{B3LYP}}}$ be, respectively, the cubic and quartic force constants calculated at the B3LYP/cc-pVTZ level, expressed in the basis of the dimensionless normal modes, calculated at the CCSD(T)/cc-pVTZ level, as

$$\phi_{ijk_{\mathrm{B3LYP}}} = \frac{\partial^3 V_{\mathrm{B3LYP}}}{(\partial q_i \partial q_j \partial q_k)_{\mathrm{CCSD(T)}}} \text{ and } \phi_{ijkl_{\mathrm{B3LYP}}} = \frac{\partial^4 V_{\mathrm{B3LYP}}}{(\partial q_i \partial q_j \partial q_k \partial q_l)_{\mathrm{CCSD(T)}}}$$

The complete anharmonic hybrid force field is obtained by the (E−G) method,[62−63] which consists of including in the same process of linear regression the values of the energy and the corresponding first analytical derivatives obtained for each point of a suitable grid.[64−65] In this way, 117 B3LYP/cc-pVTZ calculations, corresponding to the distorted geometries, are necessary to determine the complete quartic force field (i.e., 358 parameters, in agreement with the coordinates in Figure 1).

Although the experimental data constitute the absolute reference, we sought at the same time the best theoretical reference than we can currently determine (in order to estimate the performance of the hybrid method). A least-squares fitting procedure using only the energy data obtained from CCSD(T) calculations was thus used to construct the anharmonic force field of acetonitrile. This complete quartic force field was determined from 717 energy calculations in the same interpolation domain. Taking into account the much lower computational cost of the DFT analytical gradient in the extended least-squares procedure and the cost of a CCSD(T) single-point calculation, the hybrid method leads overall to a factor of 10 improvement in efficiency for determining all non-null quadratic, cubic, and quartic potential energy terms, relative to a complete set of energy calculations at the CCSD(T) level.

The vibrational energy transitions obtained from the two force fields, in the range of 300−3000 cm^{-1}, have been compared and give very similar results. Therefore, only the results of the hybrid method are presented in this paper. The complete CCSD-(T) results are discussed only in cases where a significant difference appears between experimental data and theoretical results obtained at the (CC//B3) hybrid level.

TABLE 1: Geometric Parameters[a] for the Optimized Structure of CH_3CN Obtained at the B3LYP/cc-pVTZ and CCSD(T)/cc-pVTZ Levels of Theory

	our work			
	CCSD(T)/ cc-pVTZ	B3LYP/ cc-pVTZ	CCSD(T)-cc-pVTZ, ref 29	exptl, ref[31]
R_{C-C}	1.467	1.455	1.466	1.457
R_{C-H}	1.090	1.089	1.089	1.087
$R_{C\equiv N}$	1.162	1.150	1.162	1.156
β_{HCC}	109.84	110.20	109.84	110.10

[a] Bond lengths given in angstroms, and angles, in degrees.

The second step of these calculations consists of solving the Schrödinger vibrational equation. In our approach, the vibrational Hamiltonian can be defined by the following expression,

$$H = \frac{1}{2!}\sum_i \varpi_{i_{\mathrm{CCSD(T)}}} p_i^2 + V_{\mathrm{hybrid}} \quad (2)$$

The initial basis is made up of products of wave functions of the one- and two-dimensional harmonic oscillators, characterized by Hermit or Laguerre polynomials, respectively:

$$\left|\Phi^{(0)}_{(V,l)_i}\right\rangle = \prod_{i=1}^{8}\left|\phi_{v_i,l_i}(q_i)\right\rangle \quad (3)$$

with $|\phi_{v_i,l_i}(q_i)\rangle \propto H_{v_i}(q_i)$ if the normal mode is nondegenerate and where l_i is not defined and $|\phi_{v_i,l_i}(q_i)\rangle \propto L_{v_i,l_i}(q_i)$ if the normal mode is doubly degenerate.

Each state i of interest is constructed as a linear combination of products of harmonic oscillators:

$$|\Psi_{(V,l)_i}\rangle = C_i^{(0)}|\Phi^{(0)}_{(V,l)_i}\rangle + \sum_j C_{ij}^{(1)}|\Phi^{(1)}_{(V,l)_j}\rangle + \sum_j C_{ij}^{(2)}|\Phi^{(2)}_{(V,l)_j}\rangle + \sum_j C_{ij}^{(3)}|\Phi^{(3)}_{(V,l)_j}\rangle + \sum_j C_{ij}^{(4)}|\Phi^{(4)}_{(V,l)_j}\rangle + \ldots \quad (4)$$

where $|\Phi^{(1)}_{(V,l)_j}\rangle$, $|\Phi^{(2)}_{(V,l)_j}\rangle$, $|\Phi^{(3)}_{(V,l)_j}\rangle$, and $|\Phi^{(4)}_{(V,l)_i}\rangle$ are the configurations that correspond to the mono, di, tri, and quadri excitations of each configuration $|\Phi^{(0)}_{(V,l)_i}\rangle$ and $C_i^{(0)}$, $C_{ij}^{(1)}$, $C_{ij}^{(2)}$, $C_{ij}^{(3)}$, and $C_{ij}^{(4)}$ are their coefficients in the development.

Here, we emphasize that the configurations j that directly interact with each configuration i via the form of the Hamiltonian considered are introduced into the variational procedure (first-order approximation). The introduction of second-order excitations (from penta to octa), taken into account here, changes the results by only a few cm^{-1}. This consideration allows the possibility of dividing the spectral range to be studied into several intervals for each of which a Hamiltonian matrix (see ref 66 for the matrix term expressions) is built following the scheme considered above.

In CH_3CN, the spectral range has been split into 10 spectral subspaces. Thus, the size of each submatrix to be diagonalized does not exceed 12 000 configurations for obtaining in fine the eigenvalues reported in the present study.

3. Results and Discussion

3.1. Structure, Quadratic Force Constants, and Harmonic Frequencies. Equilibrium structures calculated at both the CCSD(T)/cc-pVTZ and B3LYP/cc-pVTZ levels are summarized in Table 1. Overall, these data are in very good agreement with

TABLE 2: Harmonic Force Constants for CH_3CN and Comparisons with the Scaled Theoretical Force Field[33] as Well as Estimated Experimental Data[34a]

force constants	CCSD(T)/B3LYP	scaled SCF ref[34]	exptl ref[35]
	A1 Symmetry		
F1 (CH_3 sym stretching)	5.281/5.260	5.265	5.334
F3 (CH_3 umbrella)	0.604/0.606	0.605	0.607
F4 (C−C stretching)	5.454/5.375	5.221	5.236
F2 (C≡N stretching)	18.212/19.608	18.592	18.40
	E Symmetry		
F5 (CH_3 asym. stretching)	5.375/5.234	5.242	5.324
F6 (CH_3 deformation)	0.552/0.544	0.535	0.539
F7 (CH_3 rocking)	0.725/0.711	0.674	0.685
F8 (N≡C−C bending)	0.344/0.382	0.353	0.370
F13	0.163/0.223	0.165	0.321
F24	−0.051/−0.023	−0.03	−0.053
F23	−0.348/−0.357	−0.349	−0.378
F56	−0.170/−0.203	−0.128	−0.137
F57	0.104/0.101	0.121	0.029
F58	−0.170/−0.179	−0.018	−0.389
F78	0.012/−0.023	−0.098	−0.084

[a] Units for force constants are stretching and stretching−stretching in mdyn $Å^{-1}$, stretching−bending in mdyn rad^{-1}, and bending and bending−bending in mdyn Å rad^{-2}.

the theoretical values obtained by Margules et al.[29] and the microwave spectroscopy data.[31] In all cases, B3LYP gives results closer to the experimental data than CCSD(T).

At the DFT level, the CC and CH bond lengths were computed to be 1.455 and 1.089 Å, respectively. These values do not deviate more than 0.002 Å from the experimental data. Comparable agreement is obtained for the bond angle HCC (110.2 vs 110.1°). The only significant difference is found in the case of the CN bond length, where the calculated value is lower than the experimental one by 0.006 Å (1.150 vs 1.156 Å). This result suggests an overestimated quadratic force constant value. The same deviation is found in the CCSD(T) optimization, except that the CN bond length is, in this case, overestimated.

Both the CCSD(T)/cc-pVTZ and B3LYP/cc-pVTZ quadratic force constant result are similar and in good agreement with the experimental data of Duncan et al.[35] With regard to the diagonal force constants, we find comparable values for all quadratic terms (Table 2). However, there are some significant small differences. Contrary to the CCSD(T) results, the symmetric stretching CH force constant is greater than the asymmetric one in the B3LYP determination, in agreement with the experimental data. However, relative to the experimental data, the CN force constant is better described in our CCSD(T) calculations. For the off-diagonal terms, our theoretical results agree, in general, both in magnitude and in sign with the experimental ones. In comparison with previous theoretical work, the most significant differences concern the off-diagonal terms where our results show large couplings between the CH_3 and the CC−N bending modes and no significant coupling between the CH_3 and the C−C stretching.

The harmonic frequencies calculated at the CCSD(T)/cc-pVTZ level are reported in Table 3 and compared with those estimated by Duncan et al.[35] An accurate estimation of the harmonic frequencies in this experiment is based on the corrections made to the fundamental transitions from the observation of the overtone bands. An additional vibrational study of the various isotopes was also carried out, which has helped to locate the isotope shifts as well as the possible resonances and consequently has improved these estimates.

TABLE 3: Calculated and Experimental Harmonic Wavenumbers[a]

	assignment		CCSD(T)cc-pVTZ	ω_{exptl}[35]
ω_1	CH_3 stretching	A_1	3065	3044
ω_2	CN stretching	A_1	2297	2294
ω_3	CH_3 deformation	A_1	1413	1418
ω_4	CC stretching	A_1	920	929
ω_5	CH_3 stretching.	E	3149	3135
ω_6	CH_3 deformation	E	1487	1478
ω_7	CH_3 rocking	E	1061	1062
ω_8	CCN bending	E	361	365

[a] In cm^{-1}.

TABLE 4: Cubic and Quartic Force Constants[a] Expressed in the Dimensionless Normal CCSD(T) Modes[b]

parameter	value	parameter	value	parameter	value	parameter	value
$\phi_{1,1,1}$	−1056.0	$\phi_{4,4,4}$	−250.9	$\phi_{1,4,5,5}$	7.5	$\phi_{3,5,6,8}$	7.6
$\phi_{1,1,2}$	−21.1	$\phi_{4,5,5}$	8.7	$\phi_{1,4,5,7}$	−10.4	$\phi_{3,5,7,8}$	−11.6
$\phi_{1,2,2}$	4.4	$\phi_{4,5,7}$	−41.2	$\phi_{1,4,6,6}$	14.8	$\phi_{3,6,6,6}$	−7.2
$\phi_{1,3,3}$	−21.0	$\phi_{4,6,6}$	8.7	$\phi_{1,4,7,8}$	−11.8	$\phi_{3,6,7,7}$	−12.8
$\phi_{1,3,4}$	−19.3	$\phi_{4,6,7}$	−13.4	$\phi_{1,5,5,5}$	268.4	$\phi_{3,7,7,7}$	24.0
$\phi_{1,5,5}$	−1143.8	$\phi_{4,7,7}$	−28.1	$\phi_{1,5,6,6}$	12.2	$\phi_{4,4,4,4}$	27.9
$\phi_{1,5,6}$	−41.6	$\phi_{4,7,8}$	13.4	$\phi_{1,5,6,8}$	8.6	$\phi_{4,4,5,7}$	−9.1
$\phi_{1,5,7}$	65.1	$\phi_{4,8,8}$	−32.8	$\phi_{1,5,7,8}$	−16.2	$\phi_{4,4,5,8}$	−8.6
$\phi_{1,5,8}$	17.8	$\phi_{5,5,5}$	−823.7	$\phi_{1,6,6,8}$	7.1	$\phi_{4,5,6,6}$	12.4
$\phi_{1,6,6}$	−48.8	$\phi_{5,6,6}$	17.6	$\phi_{1,7,7,7}$	14.1	$\phi_{4,5,6,8}$	10.8
$\phi_{1,6,7}$	42.6	$\phi_{5,6,7}$	−16.4	$\phi_{2,2,2,2}$	109.9	$\phi_{4,5,7,8}$	−19.5
$\phi_{1,6,8}$	9.7	$\phi_{5,7,7}$	21.0	$\phi_{2,2,2,4}$	31.9	$\phi_{4,6,6,8}$	7.0
$\phi_{1,7,7}$	−103.3	$\phi_{5,7,8}$	9.0	$\phi_{2,2,3,3}$	−8.1	$\phi_{4,7,7,7}$	11.4
$\phi_{1,7,8}$	−15.9	$\phi_{6,6,6}$	138.7	$\phi_{2,2,4,4}$	7.2	$\phi_{5,5,5,5}$	594.6
$\phi_{2,2,2}$	−606.0	$\phi_{6,6,7}$	−40.4	$\phi_{2,2,6,6}$	−12.5	$\phi_{5,5,5,6}$	12.8
$\phi_{2,2,3}$	17.1	$\phi_{6,7,7}$	−41.4	$\phi_{2,2,7,7}$	−11.0	$\phi_{5,5,5,7}$	−19.6
$\phi_{2,2,4}$	−192.9	$\phi_{6,7,8}$	−7.1	$\phi_{2,2,7,8}$	7.6	$\phi_{5,5,7,7}$	−11.2
$\phi_{2,3,3}$	20.7	$\phi_{6,8,8}$	−7.6	$\phi_{2,4,4,4}$	−7.2	$\phi_{5,6,6,6}$	14.6
$\phi_{2,3,4}$	−37.8	$\phi_{7,7,7}$	−74.6	$\phi_{2,4,5,7}$	−7.5	$\phi_{5,6,6,7}$	−8.5
$\phi_{2,4,4}$	99.2	$\phi_{7,7,8}$	−18.5	$\phi_{2,4,6,6}$	9.1	$\phi_{5,6,7,7}$	7.9
$\phi_{2,5,5}$	−24.6	$\phi_{7,8,8}$	−5.7	$\phi_{2,4,7,7}$	8.6	$\phi_{5,6,7,8}$	8.1
$\phi_{2,5,7}$	11.0	$\phi_{1,1,1,1}$	298.1	$\phi_{2,5,7,8}$	−8.2	$\phi_{5,7,7,7}$	11.0
$\phi_{2,6,6}$	−10.1	$\phi_{1,1,1,2}$	7.3	$\phi_{2,7,7,7}$	8.1	$\phi_{5,7,7,8}$	−13.3
$\phi_{2,7,8}$	7.8	$\phi_{1,1,1,3}$	11.3	$\phi_{3,3,3,3}$	−77.8	$\phi_{5,7,8,8}$	−8.2
$\phi_{2,8,8}$	−11.2	$\phi_{1,1,5,5}$	350.2	$\phi_{3,3,3,4}$	10.2	$\phi_{5,8,8,8}$	−8.2
$\phi_{3,3,3}$	120.0	$\phi_{1,1,5,6}$	15.0	$\phi_{3,3,6,7}$	14.6	$\phi_{6,6,6,6}$	18.5
$\phi_{3,3,4}$	42.6	$\phi_{1,1,5,7}$	−11.9	$\phi_{3,3,7,7}$	−17.6	$\phi_{6,6,6,7}$	−13.0
$\phi_{3,4,4}$	79.2	$\phi_{1,1,5,8}$	−7.1	$\phi_{3,4,5,7}$	−8.8	$\phi_{6,6,7,7}$	18.0
$\phi_{3,5,5}$	−19.1	$\phi_{1,2,5,5}$	9.7	$\phi_{3,4,5,8}$	−7.3	$\phi_{7,7,7,7}$	−23.7
$\phi_{3,5,7}$	−38.6	$\phi_{1,3,3,3}$	−7.0	$\phi_{3,4,6,6}$	9.7	$\phi_{8,8,8,8}$	19.3
$\phi_{3,5,8}$	−6.8	$\phi_{1,3,5,5}$	13.6	$\phi_{3,4,7,7}$	11.4		
$\phi_{3,6,6}$	−21.5	$\phi_{1,3,5,7}$	−7.8	$\phi_{3,4,7,8}$	−7.7		
$\phi_{3,7,8}$	9.4	$\phi_{1,3,6,6}$	10.8	$\phi_{3,5,5,5}$	9.8		
$\phi_{3,8,8}$	11.8	$\phi_{1,4,4,4}$	9.0	$\phi_{3,5,6,6}$	8.6		

[a] In cm^{-1}. [b] Only the constants higher than 7 cm^{-1} are reported.

Table 3 shows the good agreement between the harmonic values calculated here and those estimated experimentally by Duncan et al.:[35] the largest deviations are 21 and 14 cm^{-1} for the two highest CH_3 stretching wavenumbers ω_1 and ω_5, or relative variations of only 0.7 and 0.4%, respectively. In the other cases, although the trend represents a more significant relative variation, it still does not exceed 1%.

3.2. Anharmonic Force Constants and Fundamental Anharmonic Wavenumbers. Table 4 reports the cubic and the quartic force constants calculated at the B3LYP/cc-pVTZ level in the dimensionless normal coordinate space defined at the CCSD(T) level.

The quartic force constants are generally smaller than the cubic terms. Only a few of them contribute significantly to the anharmonicity of the CH_3CN modes. One may especially note the active participation of the quartic force constant related to the ν_{CH} stretching modes (ϕ_{5555} = 594.6 cm^{-1}, ϕ_{1155} = 350.2 cm^{-1}, ϕ_{1111} = 298.1 cm^{-1}) and somewhat less significantly the

quartic force constants related to the ν_{CN} stretching mode ($\phi_{2222} = 109.9$ cm^{-1}), to the symmetric angular methyl deformation ($\phi_{3333} = -77.8$ cm^{-1}), and to the CH_3 rocking motion (mode number 7).

The strong interaction between modes ν_1 and ν_5 is also observed through the off-diagonal quartic constants where the term $\phi_{1555} = 268.4$ cm^{-1} leads to a significant Darling−Dennisson resonance by coupling the first harmonics of these two modes (i.e., $2\nu_5^{\pm 2} + \nu_1$ and $2\nu_1 + \nu_5^{\pm 1}$).

As for the quartic terms, the cubic terms are marked by large constant values that develop for the stretching modes of both the CH ($\phi_{111} = -1056.0$ cm^{-1}, $\phi_{155} = -1143.8$ cm^{-1}, $\phi_{555} = -823.7$ cm^{-1}) and the CN ($\phi_{222} = -606$ cm^{-1}) bonds. Except for ϕ_{224} (-192.9 cm^{-1}), ϕ_{244} (99.2 cm^{-1}), and ϕ_{177} (-103.3 cm^{-1}), the off-diagonal constants are smaller, with a few terms ranging from 35 to 100 cm^{-1}. To detect the dominant Fermi-type couplings more precisely, we can in a first analysis take into account the results given in Table 4 where we observe that the ϕ_{224} and ϕ_{244} terms are in fact not very significant because of the large gap between ν_2 and ν_4. However, the ϕ_{234} force constant, estimated to be -37.8 cm^{-1}, may be at the origin of a large splitting of the vibrational spectrum of CH_3CN due to the closeness of the two modes, ν_2 and $\nu_3 + \nu_4$. This observation confirms the experimental assumptions of Duncan et al.,[35] Bertran et al.,[41] and Mckean et al.[46] Morever, presumably the resonance between the two modes ν_6 and $\nu_7 + \nu_8$ can be explained only by large term values, such as the ϕ_{678} coefficient estimated to be 26 cm^{-1} in experiments.[52] This result is not observed, however, in our ϕ_{678} estimation because it is calculated to be only -7.1 cm^{-1}. The value obtained at the CCSD(T) level (-8.2 cm^{-1}) leads to the same conclusion.

3.3. Complete Anharmonic Spectra between 300 and 3200 cm^{-1}. The CH_3CN molecule (C_{3v}) has A_1 and E symmetry modes active in IR and Raman spectroscopy. The corresponding spectra thus present many very close bands in certain spectral areas, which does not facilitate their assignment.

The first set of experiments with acetonitrile was carried out on broad spectral ranges. These experiments were continued in more restricted ranges to observe the rotational states associated with the vibrational transitions (noted $\nu^l_{v_{J,K}}$). The states considered in our calculations correspond to the vibrational states (noted $\nu^l_{v_{0,0}}$) observed directly or estimated in experiments by linear regression of the rotational progressions observed. When these progressions are disturbed, generally by a Fermi or Coriolis resonance, empirical models are generally used to help the process of experimental interpretation. The difficulty for the spectroscopist lies in how to determine the nature of the couplings intervening among the rotational series so as to assign states $\nu^l_{v_{0,0}}$ correctly. The four spectral ranges listed in the literature are 850−1150, 1250−1450, 2250−2500, and 2950−3050 cm^{-1} including the two ν_1 and ν_5 modes.

Table 5 provides the vibrational transitions calculated by the variational method presented previously. Only the frequencies determined in several gas-phase experiments are presented in this Table for comparison. The calculated values for the unobserved or unassigned vibrational transitions are listed in Table 6.

Range 850−1150 cm^{-1}. In this area, six bands involving ν_4, $\nu_7^{\pm 1}$, $2\nu_8^0$, $2\nu_8^{\pm 2}$, $3\nu_8^{\pm 1}$, and $3\nu_8^{\pm 3}$ were studied by Tolonen et al. in 1993.[47] Although the first four modes are correctly represented by our theoretical approach, which puts them within less than 8 cm^{-1} of the observed frequencies, such is not the case for the second overtone $3\nu_8$. A possible explanation is the fact that these transitions are not observed but only estimated on the basis of the knowledge of the couplings between ν_4 and the $3\nu_8^{\pm 3}$ and/or $\nu_7^{\pm 1}$ and/or $3\nu_8^{\pm 1}$ modes. The experimental estimates led to the values of 1077 cm^{-1} for $3\nu_8^{\pm 1}$ and 1122 cm^{-1} for $3\nu_8^{\pm 3}$ (i.e., a gap of 45 cm^{-1} between the two components). This variation seems incorrect considering the low value of the coupling terms evaluated in experiments ($W_{4888} = 0.38$ cm^{-1}, $W_{7888} = 1.7$ cm^{-1}).[1] The coupling terms calculated in our theoretical approach are in perfect agreement with those given in experiments, but the shift calculated between the $3\nu_8^{\pm 1}$ (1094 cm^{-1}) and $3\nu_8^{\pm 3}$ (1098 cm^{-1}) bands is only 4 cm^{-1}. This result is in perfect agreement with the shift calculated at the CCSD(T) level, where the relative position of the two modes is overall 15 cm^{-1} lower than in the case of the hybrid method. In our opinion, the experimental band[47] at 1122 cm^{-1} cannot be assigned to the $3\nu_8^{\pm 3}$ vibration.

Range 1250−1450 cm^{-1}. Paso et al.[52] identified in this spectral range six $\nu^l_{v_{0,0}}$ transitions involving modes $\nu_8^{\pm 1} + \nu_4$, ν_3, $\nu_8^{\pm 1} + \nu_7^{\mp 1}$, $\nu_8^{\pm 1} + \nu_7^{\pm 1}$, $\nu_6^{\pm 1}$, and $4\nu_8^{\pm 2}$. Among them, frequencies $\nu_6^{\pm 1}$ and $\nu_8^{\pm 1} + \nu_7^{\pm 1}$, observed at 1450 and 1409 cm^{-1}, respectively, are coupled only in rotational levels $K = 3$ and 4. The $\nu_8^{\pm 1} + \nu_7^{\pm 1}$ mode is correctly calculated in our approach because it differs by less than 10 cm^{-1} from the

TABLE 5: Calculated Vibrational Transitions of CH_3CN between 300 and 3200 cm^{-1} and Comparison with the Experimental Data

mode	symmetry	CC//B3	CCSD(T)	exptl values
ν_8^{+1}	E	366	364	362,[36] 365[53]
$2\nu_8^0$	A_1	725	719	717[36,47]
$2\nu_8^{\pm 2}$	E	731	725	739[47]
ν_4	A_1	916	913	916,[36] 920[47]
$\nu_7^{\pm 1}$	E	1038	1038	1041,[36] 1042[47]
$3\nu_8^{\pm 1}$	E	1094	1079	1077[47,a]
$3\nu_8^{\pm 3}$	A_1, A_2	1098	1086	1122[47,a]
$\nu_8^{\pm 1} + \nu_4$	E	1282	1272	1290[52]
$\nu_8^{\pm 1} + \nu_7^{\mp 1}$	A_1, A_2	1398	1391	1402[52]
$\nu_8^{\pm 1} + \nu_7^{\pm 1}$	E	1401	1398	1410,[35] 1409[52]
ν_3	A_1	1400	1376	1390,[35,a] 1385[52,a]
$4\nu_8^{\pm 2}$	E	1467	1456	1448[52,a]
$\nu_6^{\pm 1}$	E	1478	1486	1453,[36] 1450[52]
$2\nu_7^0$	A_1	2059	2053	2075[36]
$2\nu_7^{\pm 2}$	E	2067	2068	2082[36]
$2\nu_8^{\pm 2} + \nu_6^{\mp 1}$	A_1, A_2	2203	2197	2192[51]
ν_2	A_1	2271	2247	2271,[45] 2267,[36] 2266,[35] 2248,[49] 2253[55]
$\nu_4 + \nu_7^{\pm 1} + \nu_8^{1\mp}$	A_1,A_2	2316	2311	2310[51]
$\nu_4 + \nu_7^{\pm 1} + \nu_8^{\pm 1}$	E	2330	2318	2334,[51] 2331[45]
$\nu_3 + \nu_4$	A_1	2315	2283	2305,[36] 2301,[45] 2297[49]
$\nu_4 + \nu_6^{\pm 1}$	E	2394	2395	2366,[51] 2370[45]
$2\nu_7^0 + \nu_8^{\pm 1}$	E	2428	2420	2448[51]
$\nu_3 + \nu_7^{\pm 1}$	E	2437	2408	2416[36]
$\nu_6^{\pm 1} + \nu_7^{\pm 1}$	E	2510	2508	2487[36]
$\nu_8^{\pm 1} + \nu_2$	E	2638	2610	2622[36]
$\nu_8^{\pm 1} + \nu_3 + \nu_4$	E	2694	2673	2664[36]
$2\nu_3$	A_1	2793	2739	2757[36]
$\nu_6^{\pm 1} + \nu_3$	E	2879	2862	2827[36]
$2\nu_6^0$	A_1	2934	2932	2869[36]
$2\nu_7^0 + \nu_4$	A_1	2970	2951	2997[50]
$2\nu_7^{\pm 2} + \nu_4$	E	2982	2963	3006[50]
ν_1	A_1	2994	2970	2954,[36] 2950[37]
$2\nu_8^0 + \nu_2$	A_1	2968	2968	2975[50]
$2\nu_8^{\pm 2} + \nu_2$	E	3001	2999	3000[50]
$\nu_5^{\pm 1}$	E	3043	3053	3009[36]
$\nu_2 + \nu_4$	A_1	3182	3157	3178[36]

[a] Estimated experimental transitions.

TABLE 6: Unassigned Experimental Vibrational Transitions of CH_3CN Calculated at the CC/B3 Level between 300 and 3000 cm^{-1}

mode	symmetry	calcd values	mode	symmetry	calcd values
$2\nu_8^0 + \nu_4$	A_1	1645.7	$3\nu_8^{\pm3} + \nu_6^{\mp1}$	E	2576.6
$2\nu_8^{\pm2} + \nu_4$	E	1647.0	$3\nu_8^{\pm1} + \nu_6^{\mp1}$	A_1, A_2	2572.5
$2\nu_8^{\pm2} + \nu_7^{\mp1}$	E	1769.3	$3\nu_8^{\pm1} + \nu_6^{\pm1}$	E	2575.5
$2\nu_8^0 + \nu_7^{\mp1}$	E	1767.4	$3\nu_8^{\pm3} + \nu_6^{\pm1}$	E	2571.4
$2\nu_8^{\pm2} + \nu_7^{\pm1}$	A_1, A_2	1761.6	$2\nu_8^{\pm2} + \nu_4 + \nu_7^{\mp1}$	E	2695.2
$\nu_3 + \nu_8^1$	E	1766.4	$2\nu_8^0 + \nu_4 + \nu_7^{\mp1}$	E	2693.8
$2\nu_4$	A_1	1833.7	$2\nu_8^{\pm2} + \nu_4 + \nu_7^{\mp1}$	A_1, A_2	2688.7
$\nu_6^{\pm1} + \nu_8^{\pm1}$	A_1, A_2	1838.2	$3\nu_4$	A_1	2719.4
$\nu_6^{\pm1} + \nu_8^{\pm1}$	E	1842.2	$\nu_8^{\pm1} + \nu_4 + \nu_6^{\mp1}$	A_1, A_2	2768.5
$\nu_7^{\mp1} + \nu_4$	E	1952.3	$\nu_8^{\pm1} + \nu_4 + \nu_6^{\pm1}$	E	2772.8
$3\nu_8^{\pm3} + \nu_4$	A_1, A_2	2010.3	$2\nu_7^{\pm2} + 2\nu_8^{\pm2}$	A_1, A_2	2794.7
$3\nu_8^{\pm1} + \nu_4$	E	2015.1	$2\nu_7^0 + 2\nu_8^{\pm2}$	E	2792.6
$3\nu_8^{\pm3} + \nu_7^{\mp1}$	E	2135.4	$2\nu_7^{\pm2} + 2\nu_8^{\pm2}$	E	2794.6
$3\nu_8^{\mp1} + \nu_7^{\mp1}$	A_1, A_2	2130.5	$2\nu_7^{\pm2} + 2\nu_8^0$	E	2799.6
$3\nu_8^{\pm1} + \nu_7^{\mp1}$	E	2134.5	$2\nu_7^0 + 2\nu_8^0$	A_1	2786.7
$3\nu_8^{\pm3} + \nu_7^{\mp1}$	E	2130.2	$\nu_8^{\mp1} + \nu_7^{\mp1} + \nu_3$	A_1, A_2	2811.7
$2\nu_8^{\pm2} + \nu_3$	E	2131.3	$\nu_8^{\pm1} + \nu_7^{\mp1} + \nu_3$	E	2815.3
$2\nu_8^0 + \nu_3$	A_1	2130.0	$2\nu_4 + \nu_7^{\mp1}$	E	2864.5
$\nu_8^{\pm1} + 2\nu_4$	E	2199.4	$\nu_8^{\pm1} + \nu_7^{1\mp} + \nu_6^{\mp1}$	E	2889.1
$2\nu \mp {}^2{}_8 + \nu_6^{\pm1}$	E	2210.4	$\nu_8^{\pm1} + \nu_7^{\mp1} + \nu_6^{\pm1}$	E	2887.5
$2\nu_8^0 + \nu_6^{\pm1}$	E	2208.3	$\nu_8^{\pm1} + \nu_7^{\mp1} + \nu_6^{\pm1}$	A_1, A_2	2883.5
$2\nu_7^{\pm2} + \nu_8^{\mp1}$	E	2433.3	$\nu_8^{\pm1} + \nu_7^{\mp1} + \nu_6^{\mp1}$	E	2886.8
$2\nu_7^{\pm2} + \nu_8^{\pm1}$	A_1,A_2	2428.8	$3\nu_8^{\pm3} + 2\nu_4$	A_1, A_2	2927.4
$3\nu_8^{\pm3} + \nu_3$	A_1,A_2	2494.8	$3\nu_8^{\pm1} + 2\nu_4$	E	2932.1
$3\nu_8^{\pm1} + \nu_3$	E	2499.5	$2\nu_6^{\pm2}$	E	2952.0
$\nu_6^{\pm1} + \nu_7^{\mp1}$	A_1,A_2	2501.6	$2\nu_7^{\pm2} + \nu_4$	E	2981.7
$2\nu_8^{\pm2} + 2\nu_4$	E	2563.9	$2\nu_7^0 + \nu_4$	A_1	2968.9
$2\nu_8^0 + 2\nu_4$	A_1	2562.8			

experimental results. However, mode $\nu_6^{\pm1}$ is less correctly estimated, with a difference of 28 cm^{-1} between the computed value and the experimental band. It should be noted that the most significant coupling constant ϕ_{678}, calculated at -7.1 cm^{-1}, is not sufficient to explain the postulated Fermi resonance.[52] No other constant of significant magnitude can explain this atypical variation.

The ν_3 frequency is estimated in experiments by the assumption of Coriolis coupling with mode $\nu_6^{\pm1}$ (1450 cm^{-1}) and Fermi coupling with the combination $\nu_8^{\pm1} + \nu_7^{\mp1}$ (1402 cm^{-1}). This experimental simulation gives 1390 cm^{-1} for the ν_3 mode and 3.3 cm^{-1} for the W_{378} term for the corresponding coupling. This observation can be confirmed by our theoretical approach that leads for the system $\nu_3/(\nu_8^{\pm1} + \nu_7^{\mp1})$ to values of 1400 and 1398 cm^{-1}, respectively, with a W_{378} term calculated to be around 3 cm^{-1}.

Band $4\nu_8^{\pm2}$ is calculated to be 1467 cm^{-1}, which is 19 cm^{-1} higher than the experimental datum estimated at 1448 cm^{-1}, starting from the fifth-order Fermi resonance $\nu_6^{\pm1}/4\nu_8^{\pm2}$ (the force constant involved is, however, estimated at an unusual value of 0.001 cm^{-1}) that we cannot calculate with our model. The mode $\nu_8^{\pm1} + \nu_4$ calculated at 1282 cm^{-1} is in very good agreement with the estimated experimental value (1290 cm^{-1}).

Range 2200−2500 cm⁻¹. This range is characterized by a Fermi resonance between the two modes ν_2 and $\nu_3 + \nu_4$, which has been the subject of several papers[35,45,54] and seems to be one of the most significant Fermi interactions in the CH_3CN spectrum.

The frequencies of these two vibrational bands were calculated, respectively, at 2271 and 2315 cm^{-1} (i.e., with variations of 0 and 10 cm^{-1}, respectively, for the experimental data). The corresponding coupling function of the cubic constant ϕ_{234} was found to be 13.3 cm^{-1}, in excellent agreement with the experimental estimates of Duncan et al.[35] ($W_{234} = 12.2$ cm^{-1}).

Nakagawa et al.[51] observed distortions of the rotational progression of the ν_2 mode. These distortions are generated by states $2\nu_8^{\pm2} + \nu_6^{\mp1}$, $\nu_4 + \nu_6^{\mp1}$, and $2\nu_7^0 + \nu_8^{\mp1}$ and also by the parallel and perpendicular components of the $\nu_4 + \nu_7 + \nu_8$ combination. The very low values of the coupling terms estimated empirically ($W_{2688} = 0.045$ cm^{-1} and $W_{2478} = 0.3$ cm^{-1}) do not modify the $\nu_{2_{0,0}}$ frequency. Our theoretical results (CC or CC//B3) confirm this trend.

In conclusion, the transitions calculated in this range show excellent agreement with the observed bands because the relative average deviation is approximately 0.5%, with a maximum of 1% for the $\nu_4 + \nu_6^{\mp1}$ overtone, which presents a gap of 24 cm^{-1} between computed and experimental values.

Range 2950−3050 cm⁻¹. In this range,[50] the fundamental methyl stretching modes (ν_1 and $\nu_5^{\pm}$) are expected at 2956 and 3009 cm^{-1}. We calculate these modes, respectively, at 2994 and 3043 cm^{-1} (i.e., at less than 1.5% error). Parallel and perpendicular components of the $2\nu_8^0 + \nu_2$, $2\nu_8^{\pm2} + \nu_2$, $2\nu_7^0 + \nu_4$, and $2\nu_7^{\pm2} + \nu_4$ overtones are calculated at 2968, 3001, 2970, and 2982 cm^{-1}, respectively, approaching all of the experimental data to within 25 cm^{-1}.

4. Conclusions

This study validates our approach to the least-squares determination of the potential function using a hybrid method coupled with a variational process in order to calculate the vibrational spectra of molecules containing more than five atoms.

We have shown in this paper, by using CH_3CN as an example, how these methods have enabled us to find and assign the majority of the observed data for this molecule, reproducing within an average error of 15 cm^{-1} the fundamental, overtone, and combination bands in the mid-IR region.

Acknowledgment. We acknowledge the Centre Informatique National de l'Enseignement Supérieur (CINES) for supporting this work. We express our sincere gratitude to Pr. Daisy Zhang and to Pr. Alain Dargelos for helpful discussion. Thanks are also due to Dr. Ross Brown for assistance regarding the reading and correction of the paper.

References and Notes

(1) Esposti, C. D.; Tamassia, F.; Puzzarini, C.; Tarroni, R.; Zelinger, *Z. Mol. Phys.* **1997**, *90*, 495.
(2) Botschwina, P. *Chem. Phys. Lett.* **1994**, *225*, 480.
(3) Tarroni, R.; Palmieri, P.; Senent, M. L.; Willets, A. *Chem. Phys. Lett.* **1996**, *257*, 23.
(4) Burger, H.; Breidung, S. M. J.; Thiel, W. *J. Chem. Phys.* **1996**, *104*, 499.
(5) Klatt, G.; Willets, A.; Handy, N. C.; Esponti, C. D. *Chem. Phys. Lett.* **1995**, *237*, 273.
(6) Hayward, J. A.; Sudarko; Hughes, J. M.; Von Nagy-Felsobuki, E. I.; Alderidge, L. P. *Mol. Phys.* **1997**, *92*, 177.
(7) Carbonniere, P.; Bégué, D.; Pouchan, C. *J. Phys. Chem. A* **2002**, *106*, 9290. Pouchan, C.; Zaki K. *J. Chem. Phys.* **1997**, *107*, 342.
(8) Martin, J. M. L; Lee, T. J.; Taylor, P. R.; François, J. *J. Chem. Phys.* **1996**, *103*, 2589.
(9) Lee, T. J.; Martin, J. M. L.; Taylor, P. R. *J. Chem. Phys.* **1995**, *102*, 254.
(10) Maslen, P. E.; Handy, N. C.; Amos, R. D.; Jayatilaka, D. *J. Chem. Phys.* **1992**, *97*, 4233.
(11) Willets, A.; Handy, N. C. *Spectrochim. Acta* **1997**, *53*, 1169.
(12) Miani, A.; Cané, E.; Palmieri, P.; Trombetti, A.; Handy, N. C. *J. Chem. Phys.* **2000**, *112*, 248.

(13) Miani, A.; Hanninen, V.; Horn, M.; Halonen, L. *Mol. Phys.* **2000**, *98*, 1737.
(14) Barone, V.; Festa, G.; Grandi, A.; Rega, N.; Sanna, N. *Chem. Phys. Lett.* **2004**, *388*, 279. Barone V. *Chem. Phys. Lett.* **2004**, *383*, 528.
(15) Buenker, R. J.; Peyerimhoff, S. D. *Theor. Chim. Acta* **1974**, *35*, 33.
(16) Ben Houria, A.; Gritli, H.; Jaidane, N.; Ben Lakdhar, Z.; Chambaud, G.; Rosmus, P. *Chem. Phys.* **2001**, *274*, 71.
(17) Raghavachari, K.; Trucks, G. W.; Pople, J. A.; Head-Gordon, M. *Chem. Phys. Lett.* **1989**, *157*, 479.
(18) Pak, Y.; Woods, R. C. *J. Chem. Phys.* **1997**, *107*, 5094.
(19) Bégué, D.; Carbonnière, P.; Pouchan, C. *J. Phys. Chem. A* **2001**, *105*, 11379.
(20) Pouchan, C.; Aouni, M.; Bégué, D. *Chem. Phys. Lett.* **2001**, *334*, 352.
(21) Zaki, K.; Gélizé-Duvignau, M.; Pouchan, C. *J. Chim. Phys. Phys.-Chim. Biol.* **1997**, *94*, 37.
(22) Parr, R. G.; Yang, W. *Density-Functional Theory of Atoms and Molecules*; Oxford University Press: New York, 1989.
(23) Janoschek, R. *Pure Appl. Chem.* **2001**, *73*, 1521.
(24) Wright, N. J.; Gerber, R. B. *J. Chem. Phys.* **2000**, *112*, 2598.
(25) Dressler, S.; Thiel, W. *Chem. Phys. Lett.* **1997**, *273*, 71.
(26) Shen, M.; Xie, Y.; Yamaguchi, Y.; Schaefer, H. F., III *J. Chem. Phys.* **1991**, *94*, 8112.
(27) Allen, W. D.; Csaszar, A. G. *J. Chem. Phys.* **1992**, *98*, 2983.
(28) Raeymaekers, P.; Figeys, H.; Geerlings, P. *J. Mol. Struct.* **1988**, *169*, 509.
(29) Margules, L.; Demaison, J.; Boggs, J. E. *Struct. Chem.* **2000**, *11*, 145.
(30) Dunning, T. H. *J. Chem. Phys.* **1989**, *90*, 1007.
(31) Le Guennec, M.; Wlodarczack, G.; Burie, J.; Demaison, J. *J. Mol. Spectrosc.* **1992**, *154*, 305.
(32) Dudev, T.; Bodava-Parvanova, P.; Pencheva, D.; Galabov, B. *J. Mol. Struct.* **1997**, *436*, 427.
(33) Tadjedine, M.; Flament, J. P. *Chem. Phys.* **2001**, *265*, 27.
(34) Hedberg, L.; Mills, I. M. *J. Mol. Spectrosc.* **2000**, *203*, 82.
(35) Duncan, J. L.; McKean, D. C.; Tullini, F.; Nivellini, G. D.; Pena, J. P. *J. Mol. Spectrosc.* **1978**, *69*, 123.
(36) Nagawa, I.; Shimanouchi, T. *Spectrochim. Acta* **1962**, *18*, 513.
(37) Kim, H. S.; Kim, K. *Bull. Korean Chem. Soc.* **1992**, *13*, 520.
(38) Ahmed, M. K.; Henry, B. R. *J. Chem. Phys.* **1987**, *87*, 3724.
(39) Matsuura, H. *Bull. Chem. Soc. Jpn.* **1971**, *44*, 2379.
(40) Lavalley, J. C.; Sheppard, N. *Spectrochim. Acta* **1972**, *28A*, 2091.
(41) Bertran, J. F.; La Serna, B.; Doerffel, K.; Dathe, K.; Kabish, G. *J. Mol. Struct.* **1982**, *95*, 1.
(42) Mori, Y.; Nagawaga, T.; Kuchitsu, K. *J. Mol. Spectrosc.* **1984**, *104*, 388.
(43) Nagawaga, J.; Yamada, K. M. T.; Winnewisser, G. *J. Mol. Spectrosc.* **1985**, *112*, 127.
(44) Wallraff, P.; Yamada, K. M. T.; Schieder, R.; Winnewisser, G. *J. Mol. Spectrosc.* **1985**, *112*, 163.
(45) Kyro, E.; Paso, R. *J. Mol. Spectrosc.* **1985**, *110*, 164.
(46) Mckean, D. C.; Machray, S. *Spectrochim. Acta* **1988**, *44*, 533.
(47) Tolonen, A. M.; Koivusaari, M.; Paso, R.; Schroderus, J.; Alanko, S.; Attila, R. *J. Mol. Spectrosc.* **1993**, *160*, 554.
(48) Deak, J. C.; Iwaki, L. K.; Dlott, D. D. *J. Phys. Chem. A* **1998**, *102*, 8193.
(49) Andrews, S. S.; Boxer, S. G. *J. Phys. Chem. A* **2000**, *104*, 11853.
(50) Huet, T. R. *J. Mol. Struct.* **2000**, *517*, 127.
(51) Nakawaga, J.; Yamada, K. M.; Winnewisser, G. *J. Mol. Spectrosc.* **1985**, *112*, 127.
(52) Paso, R.; Antilla, R.; Koivusaari, M. *J. Mol. Spectrosc.* **1994**, *165*, 470.
(53) Koivusaari, M.; Horneman, V. M.; Antilla, R. *J. Mol. Spectrosc.* **1992**, *152*, 377.
(54) Bertran, J. F.; La Serna, N.; Doerffel, K.; Dathe, K.; Kabish, G. *J. Mol. Struct.* **1982**, *95*, 1.
(55) Zhao, W.; Murdoch, K. M.; Besemann, D. M.; Condon, N. J.; Meyer K. A.; Wright J. C. *Appl. Spectrosc.* **2000**, *54*, 1000.
(56) Becke, A. D. *J. Chem. Phys.* **1993**, *98*, 5648.
(57) Lee, C.; Yang, W.; Parr, R. G. *Phys. Rev. B* **1988**, *37*, 785.
(58) Frisch, M. J.; Trucks, G. W.; Schlegel, H. B.; Scuseria, G. E.; Robb, M. A.; Cheeseman, J. R.; Zakrzewski, V. G.; Montgomery, J. A., Jr.; Stratmann, R. E.; Burant, J. C.; Dapprich, S.; Millam, J. M.; Daniels, A. D.; Kudin, K. N.; Strain, M. C.; Farkas, O.; Tomasi, J.; Barone, V.; Cossi, M.; Cammi, R.; Mennucci, B.; Pomelli, C.; Adamo, C.; Clifford, S.; Ochterski, J.; Petersson, G. A.; Ayala, P. Y.; Cui, Q.; Morokuma, K.; Malick, D. K.; Rabuck, A. D.; Raghavachari, K.; Foresman, J. B.; Cioslowski, J.; Ortiz, J. V.; Stefanov, B. B.; Liu, G.; Liashenko, A.; Piskorz, P.; Komaromi, I.; Gomperts, R.; Martin, R. L.; Fox, D. J.; Keith, T.; Al-Laham, M. A.; Peng, C. Y.; Nanayakkara, A.; Gonzalez, C.; Challacombe, M.; Gill, P. M. W.; Johnson, B. G.; Chen, W.; Wong, M. W.; Andres, J. L.; Head-Gordon, M.; Replogle, E. S.; Pople, J. A. *Gaussian 98*, revision A.7; Gaussian, Inc.: Pittsburgh, PA, 1998.
(59) Simons, G.; Parr, R. G.; Finlan, J. M. *J. Chem. Phys.* **1973**, *59*, 3229.
(60) Meyer, W.; Botschwina, P.; Burton, P. G. *J. Chem. Phys.* **1986**, *84*, 891.
(61) Henry, L.; Amat, G. *J. Mol. Spectrosc.* **1960**, 5, 319. Henry, L.; Amat, G. *J. Mol. Spectrosc.* **1965**, *15*, 168.
(62) Carbonniere, P.; Bégué, D.; Dargelos, A.; Pouchan, C. In *Computational Methods in Sciences and Engineering*; Simos, T. E.; Ed. World Scientific: River Edge, NJ, 2003; p 99.
(63) REGRESS EGH, Carbonniere, P.; Bégué, D.; Dargelos, A.; Pouchan C. Laboratoire de Chimie Théorique et Physico-Chimie Moléculaire, UMR CNRS 5624. IPREM FR 5626.
(64) Box, G. E. P.; Behnken, D. W. *Ann. Mater. Stat.* **1960**, *31*, 838.
(65) Carbonnière, P.; Bégué, D.; Dargelos, A.; Pouchan, C. *Chem. Phys.* **2004**, *300*, 41. Carbonnière, P.; Bégué, D.; Pouchan, C. *Chem. Phys.* **2004**, *393*, 92.
(66) Carbonnière P. Ph.D. Thesis 2001, Laboratoire de Chimie Théorique et Physico-Chimie Moléculaire, UMR CNRS 5624. IPREM FR 5626.